JOURNAL OF COMPUTATIONAL PHYSICS 92, 273–295 (1991)

On Godunov-Type Methods near Low Densities

B. EINFELDT*

College of Aeronautics, Cranfield Institute of Technology, Cranfield, Bedford, MK43 OAL, England

C. D. MUNZ

Institut für Neutronenphysik und Reaktortechnik, Kernforschungszentrum Karlsruhe, Postfach 3640, D-7500 Karlsruhe, Germany

P. L. ROE†

College of Aeronautics, Cranfield Institute of Technology, Cranfield, Bedford, MK43 OAL, England

AND

B. SJÖGREEN

University of Uppsala, Department of Scientific Computing, Sturegatan 4B, S-75223 Uppsala, Sweden

Received June 27, 1989; revised December 7, 1989

When the energy of a flow is largely kinetic, many conservative differencing schemes may fail by predicting non-physical states with negative density or internal energy. We describe as positively conservative the subclass of schemes that by contrast always generate physical solutions from physical data and show that the Godunov method is positively conservative. It is also shown that no scheme whose interface flux derives from a linearised Riemann solution can be positively conservative. Classes of data that will bring about the failure of such schemes are described. However, the Harten–Lax–van Leer (HLLE) scheme is positively conservative under certain conditions on the numerical wavespeeds, and this observation allows the linearised schemes to be rescued by modifying the wavespeeds employed.

1. INTRODUCTION

Highly energetic flows often contain regions in which the dominant energy mode is kinetic. If this kinetic energy is computed from a conservative numerical

* Work supported by a NATO research-scholarship. Present address: Konrad-Zuse-Zentrum für Informationstechnik, Heilbronner Strasse-10, D-1000 Berlin 31, Germany.

† Present address: Department of Aerospace Engineering, University of Michigan, Ann Arbor, MI 48109.

0021-9991/91 $3.00

approximation for the conservation laws of mass and momentum and then subtracted from a conservative approximation of the conservation law for the total energy, then the resulting internal energy may be negative. This of course leads to a failing of the numerical scheme. Attempting to replace negative internal energy values by positive ones leads to a non-conservative scheme and may result in a wrong shock position or an exponential error growth. Considerable importance attaches therefore to any numerical scheme for which the internal energy and density remain positive throughout the computational process. We will denote such schemes as positively conservative. In this paper we establish that for the Euler equations of gas dynamics, involving problems in any number of space dimensions: (a) Godunov's scheme [4] is positively conservative; (b) no Godunov-type scheme based on a linearized Riemann solution is positively conservative; and (c) that the HLLE-scheme [6, 2] is positively conservative, provided the absolute value of the maximal and minimal wavespeeds satisfy certain stability bounds. The results obtained in [2] also indicate how to "fix up" the methods studied under (b).

For simplicity, we present all our results for a two-dimensional setting, but they extend to three dimensions. Our theoretical arguments are based on the fact that every considered scheme derives its updated values from a convex averaging process, applied to the states that appear in the exact or approximate solution of a Riemann problem at the cell interfaces. This implies that an approximate Riemann solver leads to a positively conservative scheme if and only if all the states generated are physically real.

Preliminaries

We consider the (Euler) equations for an inviscid compressible flow. The conservation form of these equations in two Cartesian space variables is

$$\frac{\partial \mathbf{w}}{\partial t}+\frac{\partial \mathbf{f}(\mathbf{w})}{\partial x}+\frac{\partial \mathbf{g}(\mathbf{w})}{\partial y}=0 \tag{1.1}$$

$$\mathbf{w}=\begin{pmatrix}\rho\\ m\\ n\\ e\end{pmatrix},\qquad \mathbf{f}(\mathbf{w})=\begin{pmatrix}m\\ m^2/\rho+p\\ mn/\rho\\ (e+p)\,m/\rho\end{pmatrix},\qquad \mathbf{g}(\mathbf{w})=\begin{pmatrix}n\\ mn/\rho\\ n^2/\rho+p\\ (e+p)\,n/\rho\end{pmatrix}. \tag{1.2}$$

Here, the density, $m=\rho u$ and $n=\rho v$ are the momenta per unit area and $e=\rho\varepsilon+\frac{1}{2}\rho(u^2+v^2)$ is the total energy per unit area. The physical variables u, v, ε are the velocities and the internal energy per unit mass. For an ideal gas, the pressure p is defined through an equation of state of the form

$$p=(\gamma-1)\,\varepsilon\rho, \tag{1.3}$$

where γ is a constant between 1 and 2.

Many of the modern shock capturing schemes contain, as an essential part, the exact or approximate solution to one-dimensional Riemann problems of the form

$$\frac{\partial \mathbf{w}}{\partial t}+\frac{\partial}{\partial \xi}\mathbf{F}(\mathbf{w})=0 \tag{1.4a}$$

$$w(\xi, 0)=\begin{cases} w_\ell & \text{for} \quad \xi<0 \\ w_r & \text{for} \quad \xi>0, \end{cases} \tag{1.4b}$$

where

$$\mathbf{F}(\mathbf{w})=n_x\mathbf{f}(\mathbf{w})+n_y\mathbf{g}(\mathbf{w}). \tag{1.5}$$

Here $\mathbf{n}=(n_x, n_y)$ is the unit normal vector at the interface which separates the states w_ℓ and w_r, $\mathbf{F}(\mathbf{w})$ is the physical flux and ξ the variable normal to the interface.

Since the Euler equations are invariant under a Galilean transformation, it is sufficient to consider the Riemann problem.

$$\frac{\partial \mathbf{w}}{\partial t}+\frac{\partial}{\partial \xi}\mathbf{f}(\mathbf{w})=0 \tag{1.6a}$$

$$w(x, 0)=\begin{cases} w_\ell & \text{for} \quad x<0 \\ w_r & \text{for} \quad x>0 \end{cases} \tag{1.6b}$$

in the x-direction.

2. Godunov's Method

We divide the time into intervals of lengths τ and let Δ be the spatial increment. The solution is to be evaluated at time $t^n=n\tau$, where n is a non-negative integer, at the spatial increments $x_i=i\Delta$, $i=\pm 1, 2, \ldots$. Let $\mathbf{v}_i^n$ denote the cell average

$$\frac{1}{\Delta}\int_{x_{i-1/2}}^{x_{i+1/2}}\mathbf{w}(x, t^n)\,dx,$$

where $x_{i+1/2}=(i+1/2)\,\Delta$. In Godunov's method [4] the cell averages are advanced in time by solving a Riemann problem at each cell interface. The approximation at the next time-level $t^{n+1}=t^n+\tau$ is then obtained by averaging; i.e.,

$$\mathbf{v}_i^{n+1}=\frac{1}{\Delta}\int_0^{\Delta/2}\boldsymbol{\omega}_{RP}^n(x/\tau; i-1/2)\,dx+\frac{1}{\Delta}\int_{-\Delta/2}^{0}\boldsymbol{\omega}_{RP}^n(x/\tau; i+1/2)\,dx, \tag{2.1}$$

where $\boldsymbol{\omega}_{RP}^n((x-x_{i+1/2})/(t-t^n); i+1/2)$ is the exact solution to the Riemann problem at the cell interface $x_{i+1/2}=(i+1/2)\,\Delta$ at time t^n. Equation (2.1) can be re-written as

$$\mathbf{v}_i^{n+1}=\mathbf{v}_i^n-\frac{\tau}{\Delta}(\hat{\mathbf{f}}_{i+1/2}^n-\hat{\mathbf{f}}_{i-1/2}^n), \tag{2.2}$$

where the numerical flux is given by

$$\hat{\mathbf{f}}^{\mathrm{God}}_{i+1/2} = \hat{\mathbf{f}}(v_i, v_{i+1}) = \mathbf{f}(\boldsymbol{\omega}_{RP}(0; i+1/2)). \tag{2.3}$$

We define the set of admissible states by

$$G = \left\{ \begin{bmatrix} \rho \\ m \\ n \\ e \end{bmatrix} \middle| \; \rho > 0 \quad \text{and} \quad 2\rho e - (m^2 + n^2) > 0 \right\}. \tag{2.4}$$

G contains all states $\mathbf{v} = (\rho, m, n, e)^{\mathrm{T}}$ with positive density and internal energy $\varepsilon = e/\rho - \frac{1}{2}(u^2 + v^2)$. Given initial states $\mathbf{v}_i^n \varepsilon G$ and if no vacuum occurs in the exact solution to the Riemann problem at the cell interfaces, then the updated value (2.1) lies again inside G. Note that G is a convex set and that the integration in (2.1) does not take us outside G. Thus we have proved that Godunov's method is positively conservative.

3. Failure of Linearizations

The theory of Godunov-type methods, i.e., of numerical methods which are based on the exact or approximate solution of a Riemann problem at cell interfaces, is well developed for scalar conservation laws on cartesian grids; see, e.g., [3]. Today we have a number of schemes for which convergence results exist [8, 1]. However, new problems can arise when these schemes are applied to non-linear hyperbolic systems of conservation laws.

The difference scheme given by Roe [9] uses an approximate solution to the Riemann problem, found by solving the linearized Euler equations. For some choices of initial data that scheme is unstable although a solution exists. It is shown in the proposition below that an instability arises with any attempt to substitute linearized solutions, because for certain data, any linearization will yield a negative density or pressure. We express this by saying that certain Riemann problems are not linearizable.

Proposition 3.1. *For the Riemann problem* (1.6) *with the initial data* $\mathbf{w}_\ell = (\rho, -m, 0, e)^{\mathrm{T}}$ *and* $\mathbf{w}_r = (\rho, m, 0, e)^{\mathrm{T}}$ *and* $m > 0$ *one can distinguish between the following three cases*:

(a) *If* $4\gamma\rho e/(3\gamma - 1) - m^2 \leqslant 0$ *a vacuum occurs in the solution.*

(b) *If* $4\gamma\rho e/(3\gamma - 1) - m^2 > 0$ *and* $(\gamma - 1)\rho e - m^2 \leqslant 0$ *the problem has a solution with positive density and internal energy, but is not linearizable.*

(c) *If* $(\gamma - 1)\rho e - m^2 > 0$ *the problem has a solution with positive density and internal energy and is linearizable.*

Proof. The condition (a) for the occurrence of a vacuum is well known and can be found in [10]. To investigate the linearization property, we solve a Riemann problem for the linear equation

$$\frac{\partial}{\partial t}\mathbf{w} + A(\hat{\mathbf{w}})\frac{\partial}{\partial x}\mathbf{w} = 0, \qquad A = \mathbf{f}_{\mathbf{w}} \tag{3.1}$$

with the special initial states $\mathbf{w}_\ell = (\rho, -m, 0, e)^{\mathrm{T}}$ and $\mathbf{w}_r = (\rho, m, 0, e)^{\mathrm{T}}$. Here $\hat{\mathbf{w}}$ is a given average value about which the conservation law is linearized. The solution consists of four states $\mathbf{w}_\ell, \mathbf{w}_1, \mathbf{w}_2, \mathbf{w}_r$. Let

$$\mathbf{R}_1 = (1, \hat{u} - \hat{c}, \hat{v}, \hat{H} - \hat{u}\hat{c})^{\mathrm{T}}, \tag{3.2a}$$

$$\mathbf{R}_2 = (1, \hat{u}, \hat{v}, (\hat{u}^2 + \hat{v}^2)/2)^{\mathrm{T}}, \tag{3.2c}$$

$$\mathbf{R}_4 = (1, \hat{u} + \hat{c}, \hat{v}, \hat{H} + \hat{u}\hat{c})^{\mathrm{T}} \tag{3.2d}$$

be the right eigenvectors of $A(\hat{\mathbf{w}})$, where $\hat{c}$ is the average sound speed and $\hat{H}$ the average total enthalpy. Define α_i $(i = 1, ..., 4)$ as the coefficients of the projection of $\mathbf{w}_r - \mathbf{w}_\ell$ onto the right eigenvector basis; i.e.

$$\mathbf{w}_r - \mathbf{w}_\ell = \alpha_1\mathbf{R}_1 + \alpha_2\mathbf{R}_2 + \alpha_3\mathbf{R}_3 + \alpha_4\mathbf{R}_4 . \tag{3.3}$$

The states, $\mathbf{w}_1$ and $\mathbf{w}_2$ are given by

$$\mathbf{w}_1 = \mathbf{w}_\ell + \alpha_1\mathbf{R}_1 \tag{3.4a}$$

and

$$\mathbf{w}_2 = \mathbf{w}_\ell + \alpha_1\mathbf{R}_1 + \alpha_2\mathbf{R}_2 + \alpha_3\mathbf{R}_3 = \mathbf{w}_r - \alpha_4\mathbf{R}_4. \tag{3.4b}$$

We have to investigate the conditions

$$\rho_1 \geqslant 0, \qquad 2\rho_1 e_1 - m_1^2 - n_1^2 \geqslant 0, \tag{3.5a}$$

and

$$\rho_2 \geqslant 0, \qquad 2\rho_2 e_2 - m_2^2 - n_2^2 \geqslant 0. \tag{3.5b}$$

The formulas for the coefficients α_i $(i = 1, ..., 4)$ are well known [9]. In our case they simplify to

$$\alpha_1 = -m/\hat{c}, \tag{3.6a}$$

$$\alpha_2 = 0 \tag{3.6b}$$

$$\alpha_3 = 2n \tag{3.6c}$$

$$\alpha_4 = m/\hat{c} \tag{3.6d}$$

and we get

$$\rho_1 = \rho - m/\hat{c}, \qquad \rho_2 = \rho - m/\hat{c} \tag{3.7}$$

and our first condition guaranteeing positive density becomes

$$\hat{c} \geqslant m/\rho. \tag{3.8}$$

In the case $n = 0$, the condition for a positive pressure in region one is

$$2e_1 - \frac{m_1^2}{\rho_1} \geqslant 0. \tag{3.9}$$

Since $m_1 = -m - (m/\hat{c})(\hat{u} - \hat{c}) = 0$ we merely obtain

$$e_1 = e - \frac{m}{\hat{c}}(\hat{h} - \hat{u}\hat{c}) = e - \frac{m}{\hat{c}} \frac{\hat{c}^2}{\gamma - 1} \geqslant 0 \tag{3.10}$$

or

$$\hat{c} \leqslant (\gamma - 1)\frac{e}{m}. \tag{3.11}$$

Thus we obtain, if both ρ_1 and p_1 are positive,

$$\frac{m}{\rho} \leqslant \hat{c} \leqslant (\gamma - 1)\frac{e}{m}$$

and this constraint can only be satisfied if

$$(\gamma - 1)\rho e - m^2 \geqslant 0. \tag{3.12}$$

This completes the proof. Note that if m is negative (compression case) the problem can be linearized, because both ρ, and e, are positive for any choice of $\hat{c}$.

Remarks. The conditions (a), (b), and (c) in Proposition 3.1 can be rewritten in terms of the Mach number, M, as

(a) $M \geqslant 2/(\gamma - 1)$;

(b) $\sqrt{2/(\gamma(3-\gamma))} \leqslant M < 2/(\gamma - 1)$;

(c) $M \leqslant \sqrt{2/(\gamma(3-\gamma))}$.

For a gas with $\gamma = 1.4$ the dangerous zone (case (b) in Proposition 3.1) is reached already at $M = 0.94$.

The reason for the failure of any linearization in one dimension is the occurrence of two rarefaction waves in the exact solution to the Riemann problem. A different

failure of linearizations can occur in the two-dimensional form (1.6) of the Euler equations and is caused by a strong shear flow in the y-component of the velocity.

PROPOSITION 3.2. *For the Riemann problem* (1.6) *with the initial data* $w_l = (\rho, -m, -n, e)^T$ *and* $w_r = (\rho, m, n, e)^T$ *with* $m \geqslant 0$ *and* $n \geqslant 0$ *we can distinguish between the three cases*:

(a) *If* $4\gamma(\rho e - \frac{1}{2}n^2)/(3\gamma - 1) - m^2 \leqslant 0$ *a vacuum occurs in the solution.*

(b) *If* $4\gamma(\rho e - \frac{1}{2}n^2)/(3\gamma - 1) - m^2 > 0$ *and*

$$\left(e - \frac{1}{2}\frac{n^2}{\rho}\right) < \sqrt{\frac{2}{\gamma - 1}}\frac{mn}{\rho} + \frac{1}{(\gamma - 1)}\frac{m^2}{\rho},$$

the problem has a solution with positive density and internal energy, but is not linearizable.

(c) *If*

$$\left(e - \frac{1}{2}\frac{n^2}{\rho}\right) > \sqrt{\frac{2}{\gamma - 1}}\frac{mn}{\rho} + \frac{1}{\gamma - 1}\frac{m^2}{\rho}$$

the problem has a solution with positive pressure and density and can also be linearized.

Proof. Since the y-component $v = n/\rho$ of the velocity is advected with the speed of the x-component $u = m/\rho$ of the velocity at the contact discontinuity, the condition (a) for the occurrence of a vacuum follows from the corresponding condition in the one-dimensional case. The necessary and sufficient condition for linearizability is that $a\ \hat{c} \geqslant m/\rho$ exists such that

$$\left\{ -\frac{\rho m}{\gamma - 1}\hat{c}^2 + \left(\rho\tilde{e} + \frac{m^2}{\gamma - 1}\right)\hat{c} - me \right\} > 0, \tag{3.13}$$

where $\tilde{e} = e - \frac{1}{2}n^2/\rho$. The quadratic polynomial in $\hat{c}$ (2.13) has real roots if and only if

$$\frac{1}{4}\left(\frac{(\gamma - 1)\tilde{e}}{m} + \frac{m}{\rho}\right)^2 - (\gamma - 1)\frac{e}{\rho} \geqslant 0. \tag{3.14}$$

If

$$\frac{(\gamma - 1)\tilde{e}}{m} + \frac{m}{\rho} < 0,$$

the roots of the polynomial (3.13) are less than m/ρ and a negative density occurs in the approximate solution. After some rearrangement the LHS of (3.14) can be expressed as the difference of two squares and it follows that (3.14) is equivalent to

$$\left(e - \frac{1}{2}n^2/\rho\right) \geqslant \sqrt{\frac{2}{\gamma - 1}}\frac{mn}{\rho} + \frac{1}{\gamma - 1}\frac{m^2}{\rho} \tag{3.15}$$

and the proof is complete.

Proposition 3.2 has a nice geometrical interpretation. The necessary and sufficient condition for the linearizability is that either $m \leqslant 0$ or $m > 0$ and

$$\left(e - \frac{1}{2}\frac{n^2}{\rho}\right) \geqslant \sqrt{\frac{2}{\gamma - 1}}\frac{mn}{\rho} + \frac{1}{\gamma - 1}\frac{m^2}{\rho}. \tag{3.16}$$

By introducing the variables,

$$\bar{m} = \frac{m}{\sqrt{\rho e}} \geqslant 0 \qquad \text{and} \qquad \bar{n} = \frac{n}{\sqrt{\rho e}} \geqslant 0, \tag{3.17}$$

Eq. (3.16) reduces to

$$1 \geqslant \sqrt{\frac{1}{\gamma - 1}}\bar{m} + \frac{1}{\sqrt{2}}\bar{n} \geqslant 0 \tag{3.18a}$$

and the condition for positive pressure in the data becomes

$$2 \geqslant \bar{m}^2 + \bar{n}^2. \tag{3.18b}$$

Furthermore, we obtain for the condition of a continuum solution

$$\frac{3\gamma - 1}{4\gamma}\bar{m}^2 + \frac{\bar{n}^2}{2} \leqslant 1. \tag{3.18c}$$

The regions defined by (3.18) are depicted in Fig. 3.1. The lower half ($n < 0$) of the figure follows from symmetry properties of the Euler equations.

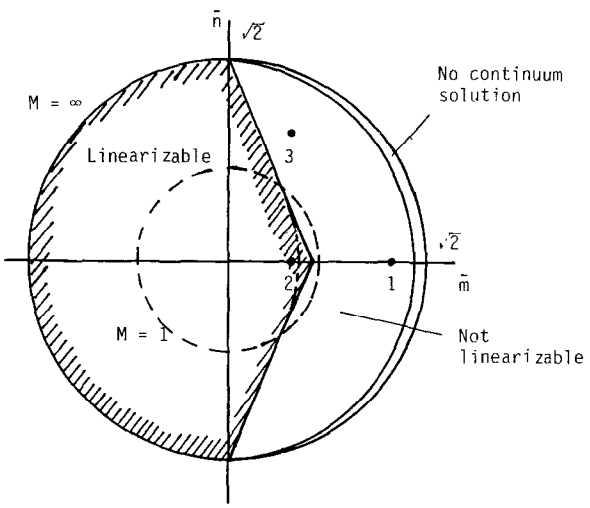

FIG. 3.1. The geometrical interpretation of Proposition 3.2. The points labelled 1, 2, 3 indicate the test problems studied in Section 6, and the small chain-dotted line shows the limits of Roe's linearisation.

It is evident from Fig. 3.1 that in most cases the failure of linearizations is caused by a shear flow in the v-component of the velocity vector; e.g., condition (c) in Proposition 2.1 applies for $\rho = 1$, $m = 1$, $n = 0$, and $e = 5$ and the solution of the Riemann problem (1.6) is linearizable, whilst for $\rho = 1$, $m = 1$, $e = 5$, and $n = 2$, condition (b) in Proposition 1.2 is satisfied and the solution of the Riemann problem (1.6) is not linearizable.

Remark. Any particular choice of linearization is valid within some subset of the indicated region in Fig. 3.1. The boundary of the subset can be found by substituting the value of $\hat{c}$ used in the linearization into Eq. (3.13) or into $\hat{c} = m/\rho$. For Roe's linearization, we have

$$\hat{c}^2 = (\gamma - 1)[\gamma e/\rho - \tfrac{1}{2}(\gamma - 1)(m^2 + n^2)/\rho^2].$$

The more restrictive condition comes from (3.13) and gives a third-order algebraic expression in $\bar{m}^2$, $\bar{n}^2$. This has been used to draw the chain-dashed line in Fig. 3.1, from which it is apparent that Roe's linearization can be applied to the great majority of linearizable problems within the category displayed.

4. The HLLE-Method

The HLLE–Riemann solver [6, 2] consists of three constant states, i.e.,

$$\omega_{\mathrm{HLLE}}(x/t; i+1/2) = \begin{cases} \mathbf{v}_i^n & \text{for } x' < b_{i+1/2}^{\ell} t \\ \mathbf{v}_{i+1/2}^n & \text{for } b_{i+1/2}^{\ell} t < x' < b_{i+1/2}^{r} t \\ \mathbf{v}_{i+1}^n & \text{for } b_{i+1/2}^{r} t < x', \end{cases} \tag{4.1}$$

where $x' = x - x_{i+1/2}$. The average state $\mathbf{v}_{i+1/2}^n$ is defined such that the Riemann solver is consistent with the integral form of the conservation law; i.e.,

$$\mathbf{v}_{i+1/2}^n = \frac{b_{i+1/2}^{\ell}\mathbf{v}_{i+1}^n - b_{i+1/2}^{\ell}\mathbf{v}_i^n}{b_{i+1/2}^{r} - b_{i+1/2}^{\ell}} - \frac{f(\mathbf{v}_{i+1}^n) - f(\mathbf{v}_i^n)}{b_{i+1/2}^{r} - b_{i+1/2}^{\ell}}. \tag{4.2}$$

Here, $b_{i+1/2}^{r}$ and $b_{i+1/2}^{\ell}$ are numerical approximations for the largest and smallest physical signal-velocities in the exact solution to the Riemann problem. Having computed the approximate solver at the cell interface, we obtain the cell average at the next time-level similar to (2.1),

$$\mathbf{v}_i^{n+1} = \frac{1}{\Delta}\int_0^{\Delta/2} \omega_{\mathrm{HLLE}}(x/\tau; i-1/2)\, dx + \frac{1}{\Delta}\int_{-\Delta/2}^{0} \omega_{\mathrm{HLLE}}(x/\tau; i+1/2)\, dx. \tag{4.3}$$

This again can be written in conservation form

$$\mathbf{v}_i^{n+1} = \mathbf{v}_i^n - \lambda\{\hat{\mathbf{f}}_{i+1/2}^n - \hat{\mathbf{f}}_{i-1/2}^n\}, \tag{4.4a}$$

with the numerical flux-function

$$\hat{\mathbf{f}}^{\mathrm{HLLE}}_{i+1/2} = \frac{b^+_{i+1/2}\mathbf{f}(\mathbf{v}_i) - b^-_{i+1/2}\mathbf{f}(\mathbf{v}_{i+1})}{b^+_{i+1/2} - b^-_{i+1/2}} + \frac{b^+_{i+1/2} \cdot b^-_{i+1/2}}{b^+_{i+1/2} - b^-_{i+1/2}} (\mathbf{v}_{i+1} - \mathbf{v}_i), \tag{4.4b}$$

where $b^+_{i+1/2} = \max\{b^s_{i+1/2}, 0\}$ and $b^-_{i+1/2} = \min\{b^\ell_{i+1/2}, 0\}$; see [2] for details.

The HLLE-scheme (4.4) with the numerical signal velocities

$$b^\ell_{i+1/2} = \min\{a^1_{i+1/2}, u_i - c_i\} \tag{4.5a}$$

and

$$b^s_{i+1/2} = \max\{a^4_{i+1/2}, u_{i+1} + c_{i+1}\}, \tag{4.5b}$$

where $a^k_{i+1/2}$ $(k = 1, ..., 4)$ are the eigenvalues of the Roe linearisation for (1.6a) and $c = (\gamma p/\rho)^{1/2}$ is the sound speed, is positively conservative. The proof is straight forward: The numerical signal velocities (4.5) are lower and upper bounds for the physical signal velocity. Therefore the average state (4.2) is given by

$$\mathbf{v}^n_{i+1/2} = \frac{1}{(b^s_{i+1/2} - b^\ell_{i+1/2})\,\tau} \int_{b^\ell_{i+1/2}\tau}^{b^s_{i+1/2}\tau} \boldsymbol{\omega}_{\mathrm{RP}}(x'/\tau; i + \tfrac{1}{2})\, dx', \tag{4.6}$$

where $\boldsymbol{\omega}_{\mathrm{RP}}(x'/\tau; i + \frac{1}{2})$ is the exact solution to the Riemann problem at the cell-interface $x_{i+1/2}$. As long as no vacuum is present, all states in the exact solution to the Riemann problem (1.6) are inside the set (2.4). Since G is convex, the averaging process (4.6) will give a value inside G. Thus the average state (4.6) is inside G. Furthermore, the solution at the next time-level t^{n+1} is obtained from the averaging process (4.3), which again will not take us outside G, since G is convex. Thus we have proved that the HLLE-scheme is positively conservative.

An enlargement of the numerical signal velocities increases the numerical dissipation in the HLLE-scheme; e.g., the numerical signal velocities

$$b^s_{i+1/2} = \{|u_{i+1/2}| + c_{i+1/2}, |u_i| + c_i, |u_{i+1}| + c_{i+1}\} \tag{4.7a}$$

$$b^\ell_{i+1/2} = -b^s_{i+1/2}, \tag{4.7b}$$

where $c_{i+1/2} = (a^4_{i+1/2} - a^1_{i+1/2})/2$ and $u_{i+1/2} = (a^4_{i+1/2} + a^1_{i+1/2})/2$, reduce (4.4b) to

$$\mathbf{f}_{i+1/2} = \tfrac{1}{2}\{\mathbf{f}(\mathbf{v}_i) + \mathbf{f}(\mathbf{v}_{i+1}) - b^s_{i+1/2}(\mathbf{v}_{i+1} - \mathbf{v}_i)\} \tag{4.8}$$

which is a numerical flux function of Lax–Friedrich type. The scheme (4.4a), (4.8) is very diffusive and gives significantly less accurate results than the scheme (4.4), (4.5).

The numerical signal velocities (4.5) can be improved concerning the numerical dissipation near rarefaction waves, subject to the restriction that the scheme (4.4)

is positively conservative. Some algebra shows that the scheme (4.4) is positively conservative if the numerical signal velocities satisfy the inequalities (see Appendix),

$$(b^{\ell}_{i+1/2} - u_i)^2 \geqslant \beta^2 c_i^2 \tag{4.9a}$$

$$(u_r - b^{r}_{i+1/2})^2 \geqslant \beta^2 c_r^2 \qquad \left(\beta^2 = \frac{\gamma - 1}{2\gamma}\right) \tag{4.9b}$$

and these results are the sharpest possible (in the one-dimensional case) for $b^{\ell}_{i+1/2} = b^{\ell}(v_i)$ and $b^{r}_{i+1/2} = b^{r}(v_{i+1})$. Hence the numerical signal velocities,

$$b^{\ell}_{i+1/2} = \min\{a^1_{i+1/2},\ u_i - \beta c_i\} \tag{4.10a}$$

$$b^{r}_{i+1/2} = \max\{a^4_{i+1/2},\ u_{i+1} + \beta c_{i+1}\}, \tag{4.10b}$$

lead to a positively conservative HLLE-scheme.

Since

$$u_i - c_i < u_i - \beta c_i \qquad \text{and} \qquad u_{i+1} + \beta c_{i+1} < u_{i+1} + c_{i+1} \tag{4.11}$$

the numerical signal velocities (4.10) decrease the dissipation for most rarefaction waves. If the states v_i and v_{i+1} are connected by a single shock wave, then the numerical signal velocities (4.5) and (4.11) reduce both to

$$b^{\ell}_{i+1/2} = a^1_{i+1/2} \qquad \text{or} \qquad b^{r}_{i+1/2} = a^4_{i+1/2}, \tag{4.12}$$

which gives the optimal numerical dissipation for a shock wave; see [2] for details.

Another problem associated with the failure of the Roe-average eigenvalues $a_{i+1/2}$ $(i = 1, \ldots, 4)$ for rarefactions was addressed in [11]. M. Vinokur observed that it is possible that the Roe average eigenvalue $a^1_{i+1/2}$ or $a^4_{i+1/2}$ could lie outside the range of values determined by $\lambda^1(v_i)$ and $\lambda^1(v_{i+1})$, respectively, $\lambda^4(v_i$ and $\lambda^4(v_{i+1})$. In particular, if the normal velocities u_i and u_{i+1} are close to the sonic speed c_i, the corresponding eigenvalues could both be of one sign, while the Roe averaged eigenvalue could have opposite signs. Assume

$$a^1_{i+1/2} < \lambda^1(v_i) \leqslant \lambda^1(v_{i+1}), \tag{4.13}$$

which holds for all the examples in [11]. In this case,

$$b^{\ell}_{i+1/2} = a^1_{i+1/2} < \lambda^1(v_i) \leqslant \lambda^1(v_{i+1}) \tag{4.14}$$

for the algorithms (4.5) and (4.10). Thus the numerical signal velocities (4.5) or (4.10) introduce more numerical dissipation into the scheme (4.4) than the physical signal speed $\lambda^1(v_i)$. However, the failure (4.13) is not significant for the scheme (4.4) and also for Roe's scheme (as we will see in the next section), because an enlargement of the numerical signal velocities retains the stability of the HLLE-scheme (4.4); see [2] for details. Furthermore, we did not observe any loss of resolution in the numerical solution through the additional numerical dissipation.

5. Some Remarks About Roe's Method

In this section we give a different simple explanation for the failure of Roe's method. A modified HLLE-scheme was proposed in [2]. The modified Riemann solver is defined by

$$\omega_{\mathrm{HLLEM}}(x'/t; i+1/2)$$

$$= \begin{cases} \mathbf{v}_i & \text{for } x' < b^{\ell}_{i+1/2} t \\ \mathbf{v}_{i+1/2} + (x - \bar{u}_{i+1/2} t)(\hat{\delta}^2_{i+1/2} \hat{\alpha}^2_{i+1/2} \hat{\mathbf{R}}^2_{i+1/2} + \hat{\delta}^3_{i+1/2} \hat{\alpha}^3_{i+1/2} \hat{\mathbf{R}}^3_{i+1/2}) & \\ & \text{for } b^{\ell}_{i+1/2} t < x' < b^{r}_{i+1/2} t \\ \mathbf{v}_{i+1} & \text{for } b^{r}_{i+1/2} t < x', \end{cases} \tag{5.1}$$

where $\hat{\mathbf{R}}^2_{i+1/2} = \hat{\mathbf{R}}^2(\hat{\mathbf{w}}_{i+1/2})$ and $\mathbf{R}^3 = \mathbf{R}^3(\hat{\mathbf{w}}_{i+1/2})$ are the second and third right eigenvectors of the Jacobian matrix $d\mathbf{f}(\hat{\mathbf{w}}_{i+1/2}) = A(\hat{\mathbf{w}}_{i+1/2})$ evaluated at an average state $\hat{\mathbf{w}}_{i+1/2} = (\hat{\rho}, \hat{u}, \hat{v}, \hat{c})^{\mathrm{T}}$. $\hat{\alpha}^2_{i+1/2} = \alpha^2(\hat{\mathbf{w}}_{i+1/2})$ and $\hat{\alpha}^3_{i+1/2} = \alpha^3(\hat{\mathbf{w}}_{i+1/2})$ are the coefficients of the projection of $(\mathbf{v}_{i+1} - \mathbf{v}_i)$ onto these eigenvectors; i.e.,

$$\mathbf{v}_{i+1} - \mathbf{v}_i = \sum_{\ell=1}^{4} \hat{\alpha}^{\ell}_{i+1/2} \hat{\mathbf{R}}^{\ell}_{i+1/2}. \tag{5.2}$$

$\hat{\delta}^2_{i+1/2}$ and $\hat{\delta}^3_{i+1/2}$ are positive parameters which control the amount of anti-diffusion in the linear degenerate fields. For $\hat{\delta}^2_{i+1/2} = 0$ and $\hat{\delta}^3_{i+1/2} = 0$, we retain the Riemann solver (4.1). Several choices for the average state $\hat{\mathbf{w}}_{i+1/2}$ are possible, we choose here

$$\hat{\rho}_{i+1/2} = \sqrt{\rho_i \rho_{i+1/2}}, \tag{5.3a}$$

$$\hat{u}_{i+1/2} = \frac{\sqrt{\rho_i}\, u_i + \sqrt{\rho_{i+1}}\, u_{i+1}}{\sqrt{\rho_i} + \sqrt{\rho_{i+1}}} \tag{5.3b}$$

$$\hat{v}_{i+1/2} = \frac{\sqrt{\rho_i}\, v_i + \sqrt{\rho_{i+1}}\, v_{i+1}}{\sqrt{\rho_i} + \sqrt{\rho_{i+1}}} \tag{5.3c}$$

$$\hat{H}_{i+1/2} = \frac{\sqrt{\rho_i}\, H_i + \sqrt{\rho_{i+1}}\, H_{i+1}}{\sqrt{\rho_i} + \sqrt{\rho_{i+1}}} \tag{5.3d}$$

$$\hat{c}^2_{i+1/2} = (\gamma - 1)\left\{ \hat{H}_{i+1/2} - \frac{1}{2}(\hat{u}^2_{i+1/2} + \hat{v}^2_{i+1/2}) \right\}. \tag{5.3e}$$

The value $\bar{u}_{i+1/2}$ in (5.1) is an approximation for the velocity at the contact discontinuity, defined by

$$\bar{u}_{i+1/2} = \frac{b^{r}_{i+1/2} + b^{\ell}_{i+1/2}}{2}. \tag{5.4}$$

The Godunov-type-scheme corresponding to the Riemann solver (5.1) can again be written in conservation form

$$\mathbf{w}^{n+1}_i = \mathbf{w}^n_i - \lambda\{\hat{\mathbf{f}}^n_{i+1/2} - \hat{\mathbf{f}}^n_{i-1/2}\} \tag{5.5a}$$

with

$$\hat{\mathbf{f}}^{\mathrm{HLLEM}}_{i+1/2} = \mathbf{f}^{\mathrm{HLLE}}_{i+1/2} - \frac{b^+_{i+1/2} \cdot b^-_{i+1/2}}{b^+_{i+1/2} - b^-_{i+1/2}} \times \{\delta^2_{i+1/2}\,\hat{\alpha}^2_{i+1/2}\mathbf{R}^2_{i+1/2} + \delta^3_{i+1/2}\hat{\alpha}^3_{i+1/2}\hat{\mathbf{R}}^3_{i+1/2}\}. \tag{5.5b}$$

The anti-diffusion coefficients in (5.1) are defined such that they take out excess dissipation in the linear degenerate fields, subject to the restriction that the stability of the HLLE-schemes is to be preserved; we set

$$\delta^2_{i+1/2} = \frac{\hat{c}_{i+1/2}}{\hat{c}_{i+1/2} + |\bar{u}_{i+1/2}|} = \delta^3_{i+1/2}. \tag{5.6}$$

It was noted in [2], that if we choose for the numerical signal velocities the largest and smallest eigenvalues of a Roe-average matrix, i.e.,

$$b^-_{i+1/2} = a^1_{i+1/2} \qquad \text{and} \qquad b^+_{i+1/2} = a^4_{i+1/2}, \tag{5.7}$$

then the HLLEM-scheme (5.5) becomes equivalent to Roe's scheme. If we apply this scheme to the initial-value problems described in Proposition 1.1, then the projection values $\hat{\alpha}^2_{i+1/2}$ and $\hat{\alpha}^3_{i+1/2}$ vanish and the HLLEM-scheme (5.5), (5.7) differs from the HLLE-scheme (4.4), (4.5) only by the definition of the numerical signal velocities. Computation of the average state (4.2), with the numerical signal velocities (5.7) may result in a negative density for the case (b) of Proposition 1.1. We obtain, furthermore, for $w_i = (\rho_i, -m_i, 0, \rho_i)^{\mathrm{T}}$ and $w_{i+1} = (\rho_{i+1}, m_{i+1}, 0, e_{i+1})^{\mathrm{T}}$.

$$u_i - c_i < a^1_{i+1/2} \qquad \text{and} \qquad a^4_{i+1/2} < u_{i+1} + c_{i+1}. \tag{5.8}$$

Thus, we conclude: The reason for the failure of Roe's method in solving case (b) of Proposition 1.1 is that the numerical signal velocities (in this case the eigenvalues of the Roe average matrix) of Roe's Riemann solver underestimates the physical signal velocities. A similar argument can be applied to the initial value problems of Proposition 1.2, if we reset the anti-diffusion coefficient $\delta^3_{i+1/2}$ to zero.

Remark. The HLLEM-scheme can be rewritten as

$$\mathbf{f}_{i+1/2} = \frac{1}{2}\left\{\mathbf{f}(\mathbf{v}_i) + \mathbf{f}(\mathbf{v}_{i+1}) - \sum_{R=1}^{4} Q^R_{i+1/2}\alpha^R_{i+1/2}R^R_{i+1/2}\right\} \tag{5.9}$$

with

$$Q^1_{i+1/2} = \frac{b^+_{i+1/2} + b^-_{i+1/2}}{b^+_{i+1/2} - b^-_{i+1/2}}\alpha^1_{i+1/2} - 2\frac{b^+_{i+1/2}b^-_{i+1/2}}{b^+_{i+1/2} - b^-_{i+1/2}} \tag{5.10a}$$

$$Q^2_{i+1/2} = \frac{b^+_{i+1/2} + b^-_{i+1/2}}{b^+_{i+1/2} - b^-_{i+1/2}}\alpha^2_{i+1/2} - 2(1-\delta^2_{i+1/2})\frac{b^+_{i+1/2}b^-_{i+1/2}}{b^+_{i+1/2} - b^-_{i+1/2}} \tag{5.10b}$$

$$Q^3_{i+1/2} = \frac{b^+_{i+1/2} + b^-_{i+1/2}}{b^+_{i+1/2} - b^-_{i+1/2}} \alpha^3_{i+1/2} - 2(1 - \delta^3_{i+1/2}) \frac{b^+_{i+1/2} b^-_{i+1/2}}{b^+_{i+1,2} - b^-_{i+1/2}} \tag{5.10c}$$

$$Q^4_{i+1/2} = \frac{b^+_{i+1/2} + b^-_{i+1/2}}{b^+_{i+1/2} - b^-_{i+1/2}} \alpha^4_{i+1/2} - 2 \frac{b^+_{i+1/2} b^-_{i+1/2}}{b^+_{i+1/2} - b^-_{i+1/2}}. \tag{5.10d}$$

The scheme (5.9) can also be considered as an improvement to Roe's original scheme. In contrast to the original Roe-scheme this scheme does not require an artificial entropy fix and does not suffer under the instabilities described in Section 3.

6. Numerical Results

The Riemann problem described in Propositions 3.1 and 3.2 occurs, e.g., when reflected boundary conditions are used at a solid wall boundary and the fluid flow is directed away from the wall. A typical example is the external flow behind an obstacle. Here starting a steady state computation by setting the initial data equal to the freestream flow field can be disastrous. In this section we show numerical results for two test problems which complement our analytical findings. First we consider a Riemann problem of the form (1.6) with the initial data $\mathbf{w}_\ell = (\rho_\ell = 1, m_\ell = 2, n_\ell = 0, e_\ell = 3)^T$ and $\mathbf{w}_r = (\rho_r = 1, m_r = 2, n_r = 0, e_r = 3)^T$. Subsequently, the problems are abbreviated by merely quoting the right-hand state vector, here (1–2–0–3) labelled 1 in Fig. 3.1. The solution of this problem consists of two rarefaction waves, one travelling to the left and one to the right. The initial data satisfy condition (b) of Proposition 3.1. The numerical results are depicted in Figs. 6.1, 6.2, and 6.3. In all calculations we used a fixed uniform grid in space with the step size $\Delta x = 0.01$. The time increment τ was calculated in each time step according to

$$\frac{\tau}{\Delta x} \max_i \{|u_i| + c_i\} \leqslant \frac{1}{2}. \tag{6.1}$$

Roe's scheme [9] explodes after a few time-steps. Figure 6.1 shows numerical results for Roe's scheme with the entropy fix proposed by Harten and Hyman [5]. The pressure and the velocity of the exact solution are represented by the solid line, the numerical approximation is represented by dots. Unphysical oscillations are visible at time $t = 0.05$. Roe's scheme with the commonly used entropy fix in [7] also fails after a few time steps. The results for the HLLE-scheme (4.4) at times $t = 0.05$ and 0.1 are depicted in Fig. 6.2. The HLLE-scheme solves this problem without any difficulties. The next figure shows the results for the HLLEM/Roe-scheme (5.9), (5.10) with the numerical signal-velocities (4.5). The results are similar to the results for the HLLE-scheme. Figures 6.4–6.6 represent the results for a Riemann problem of the form (1.6) with the initial data $w_\ell = (\rho_\ell = 1, m_\ell = -1, n_\ell = n, e_\ell = 5)^T$ and $w_r = (\rho_r = 1, m_r = 1, n_r = n, e_r = 5)^T$. The exact solution consists

of two rarefaction waves moving in opposite directions, separated by a shear flow in the y-direction. The initial data with $n=0$ satisfy condition (c) of Proposition 1.1 (point 2 in Fig. 3.1). All of our schemes solved this problem without real difficulty, although Fig. 6.4 shows some not entirely smooth behaviour in the density. However, for the same test problem with $n=2$ (point 3 in Fig. 3.1), Roe's scheme explodes after a few time-steps. This is caused by the presence of shear flow; see Proposition 3.2b. The results for the HLLE-scheme and the modified HLLE-scheme

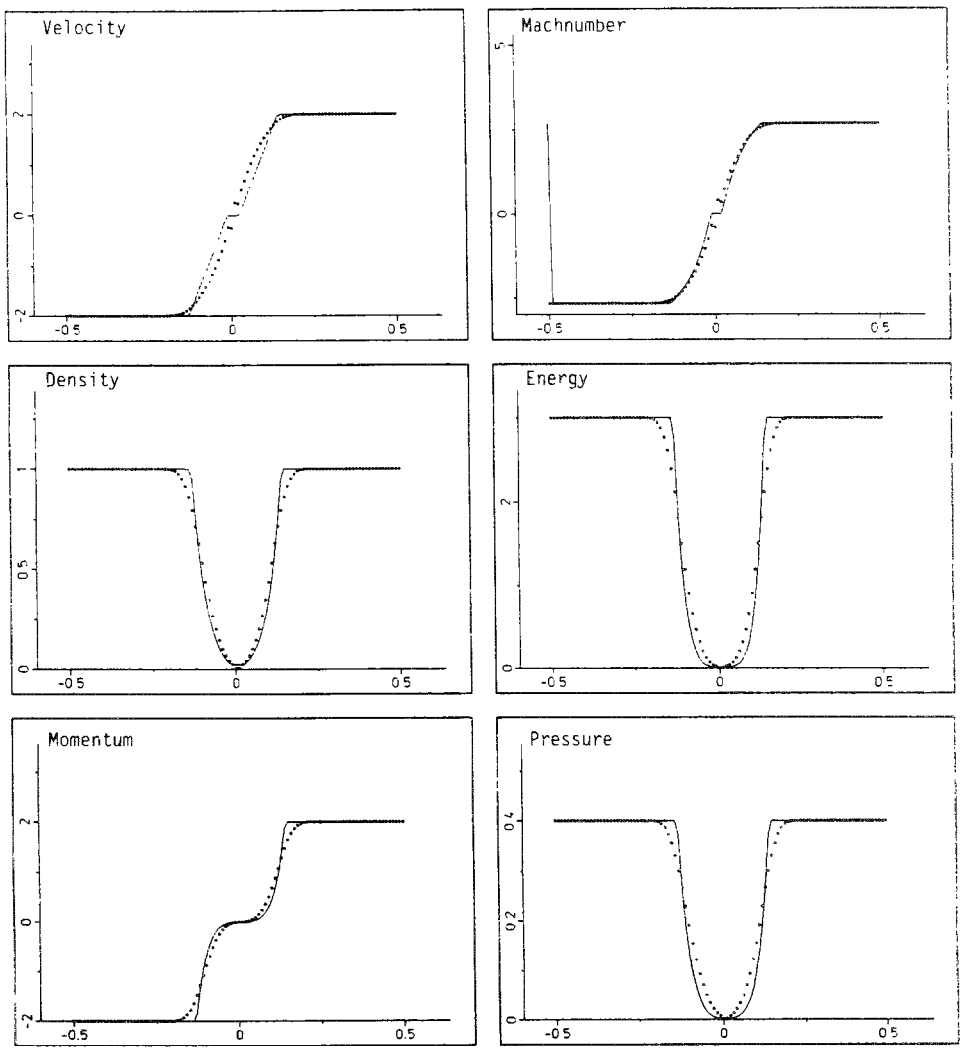

FIG. 6.1. Numerical result of Roe's scheme with the entropy fix in [5] for the 1–2–0–3 problem at time $t=0.05$.

with $\delta^3_{i+1/2}$ reset to zero are shown in Figs. 6.5 and 6.6. Both schemes solved this test problem without breaking down, but the results from the unmodified scheme are better behaved.

Concluding Remarks

Considerable importance attaches to any numerical scheme for which the internal energy and density remains positive during the computational process. It was

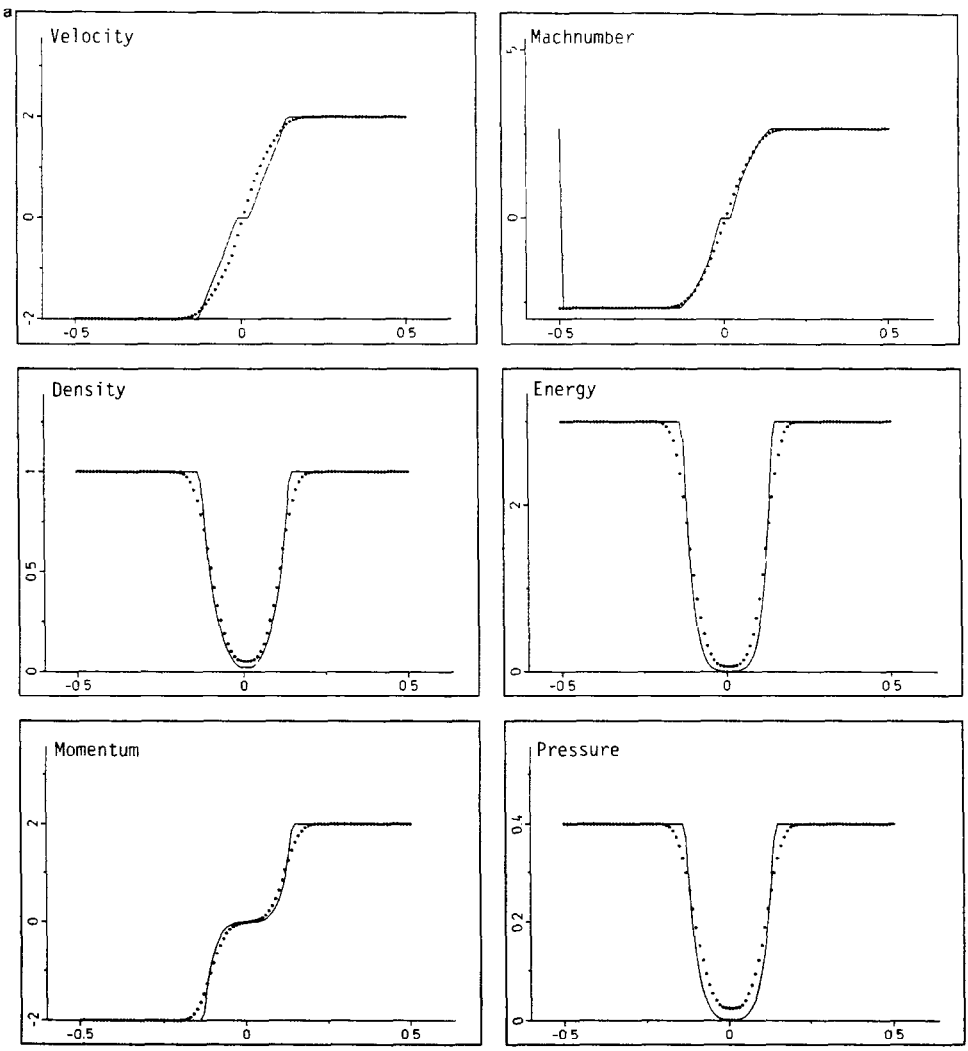

FIG. 6.2a. Numerical result of the HLLE-scheme for the 1–2–0–3 problem at time $t = 0.05$.

proved that Godunov's and the HLLE-scheme have this property, whilst schemes which are based on a local linearized Riemann solver (e.g., Roe's scheme) may lead to an unphysical negative density or internal energy during the computational process. The interpretation of Roe's scheme as an HLLE-scheme with the appropriate anti-diffusion term in the linear degenerate field leads to an improved scheme, which does not require an artificial entropy fix and does not suffer from the instabilities described in Section 3. The form (5.9) of this HLLEM-scheme can be used to fix up computer programs, which are based on the original Roe-scheme. These results open the way for the application of a class of conservative differencing

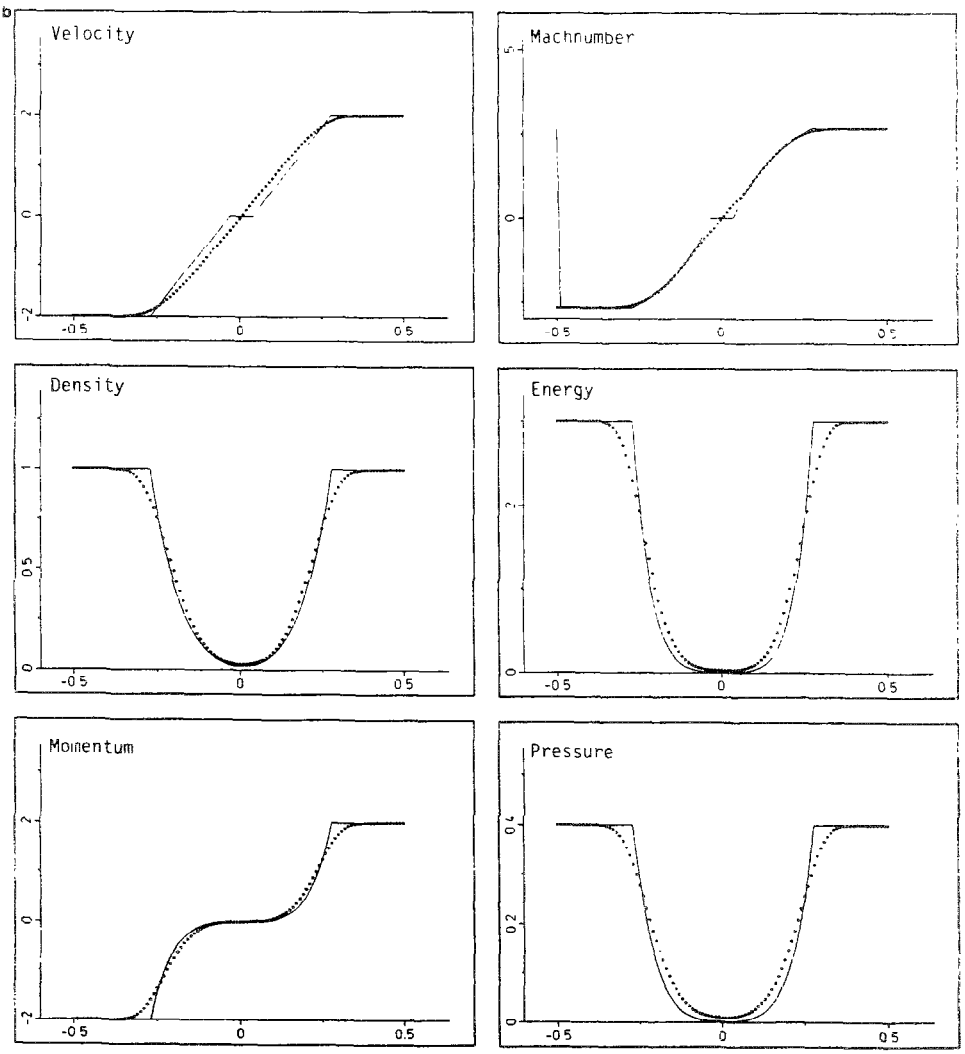

FIG. 6.2b. Numerical result of the HLLE-scheme for the 1–2–0–3 problem at time $t = 0.1$.

schemes in contexts where they have previously been regarded with suspicion. Nevertheless, all our results are only first-order accurate as yet, and there is still work to do in achieving consistently high-quality solutions.

APPENDIX: PROOF OF THE POSITIVITY CONDITION (4.9)

Each conserved variable q_i in the central zone of the HLLE-Riemann solver (4.1) is given by

$$q^* = \frac{b^r q^r - b^\ell q_\ell}{b^r - b^\ell} - \frac{f_r - f_\ell}{b^r - b^\ell}. \tag{A1}$$

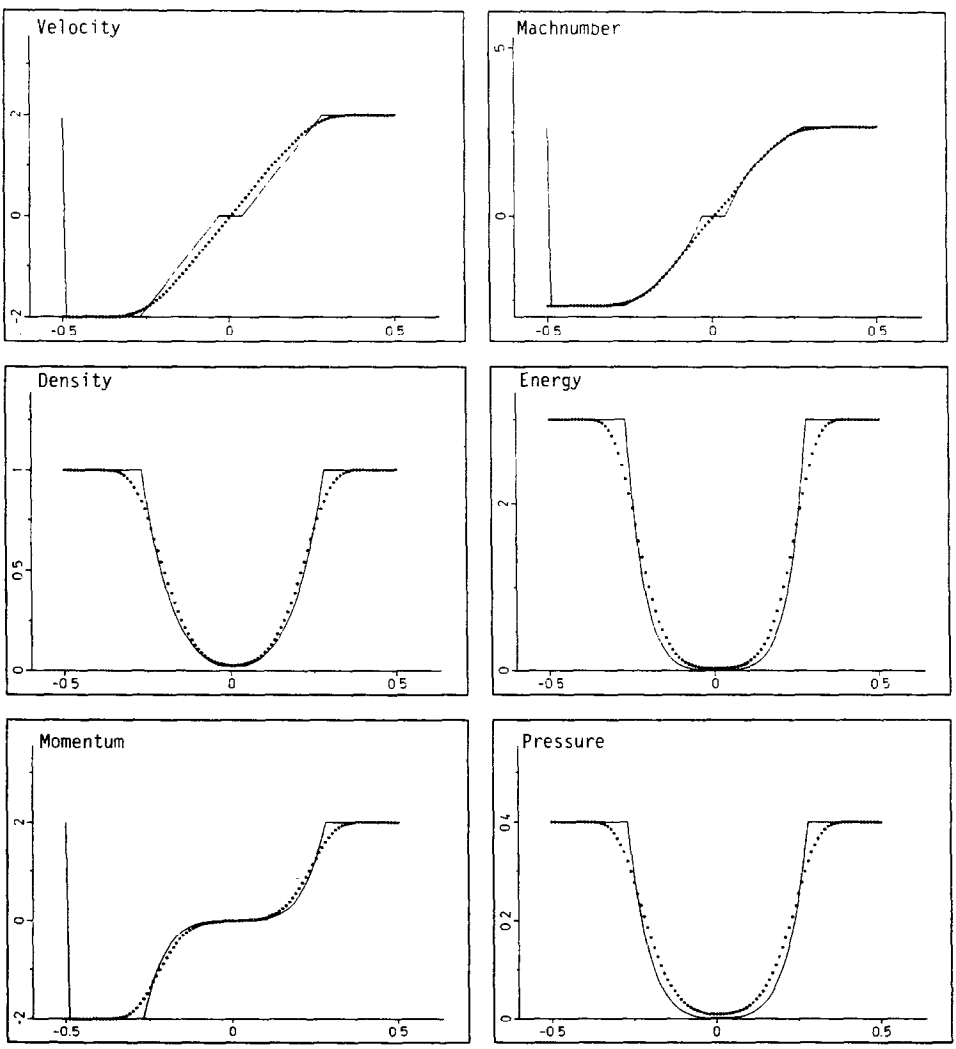

FIG. 6.3. Numerical result of the HLLEM/Roe-scheme for the 1–2–0–3 problem of time $t = 0.1$.

We omitted the subscript $i+1/2$ and set $q_r = q_{i+1}$, $q_\ell = q_i$. We obtain for the density

$$\rho^* = \frac{a_r \rho_r + a_\ell \rho_\ell}{b_r - b_\ell}, \tag{A2}$$

where we have used the abbreviations

$$a_r = b_r - u_r \qquad \text{and} \qquad a_\ell = u_\ell - b_\ell. \tag{A3}$$

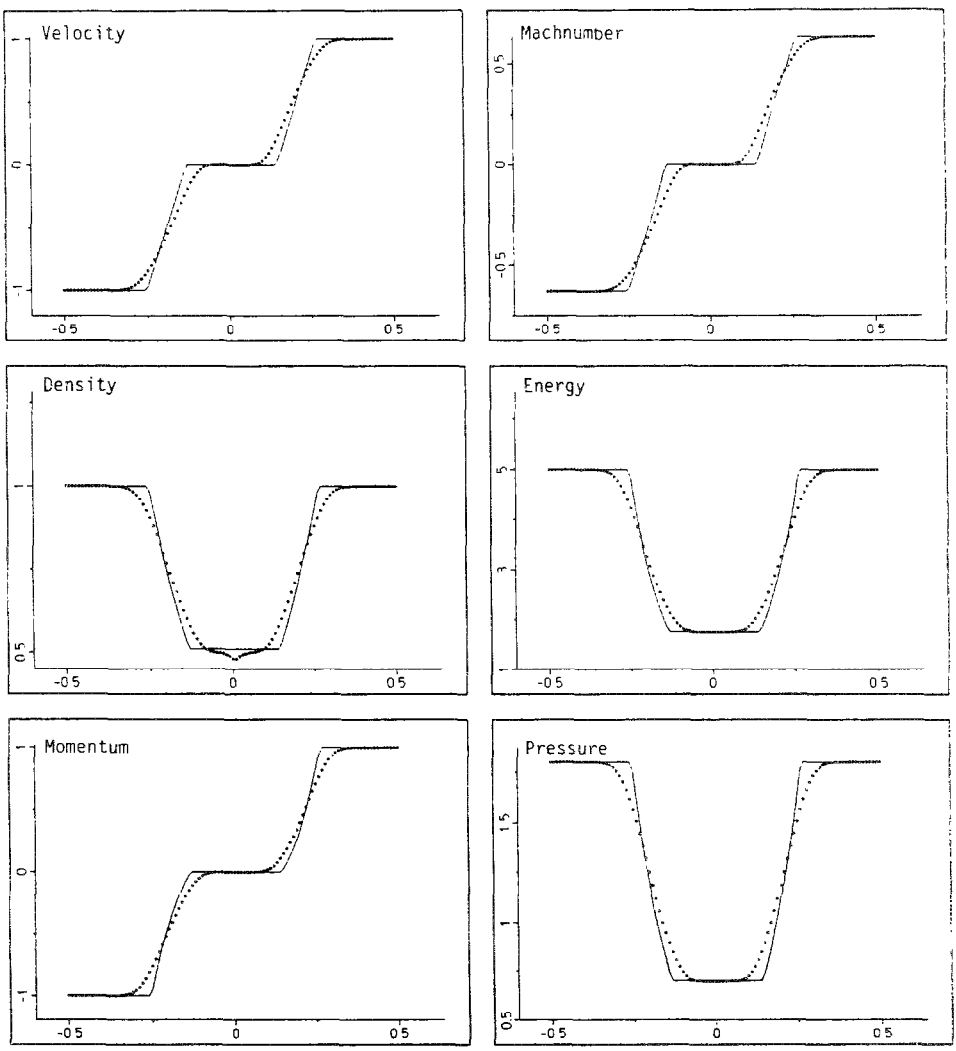

FIG. 6.4. Numerical result of Roe's scheme for the 1–1–0–5 problem at time $t = 0.1$.

Sufficient conditions for positive density are

$$a_s, a_\ell \geqslant 0 \tag{A4}$$

and

$$b_s - b_\ell \geqslant 0. \tag{A5}$$

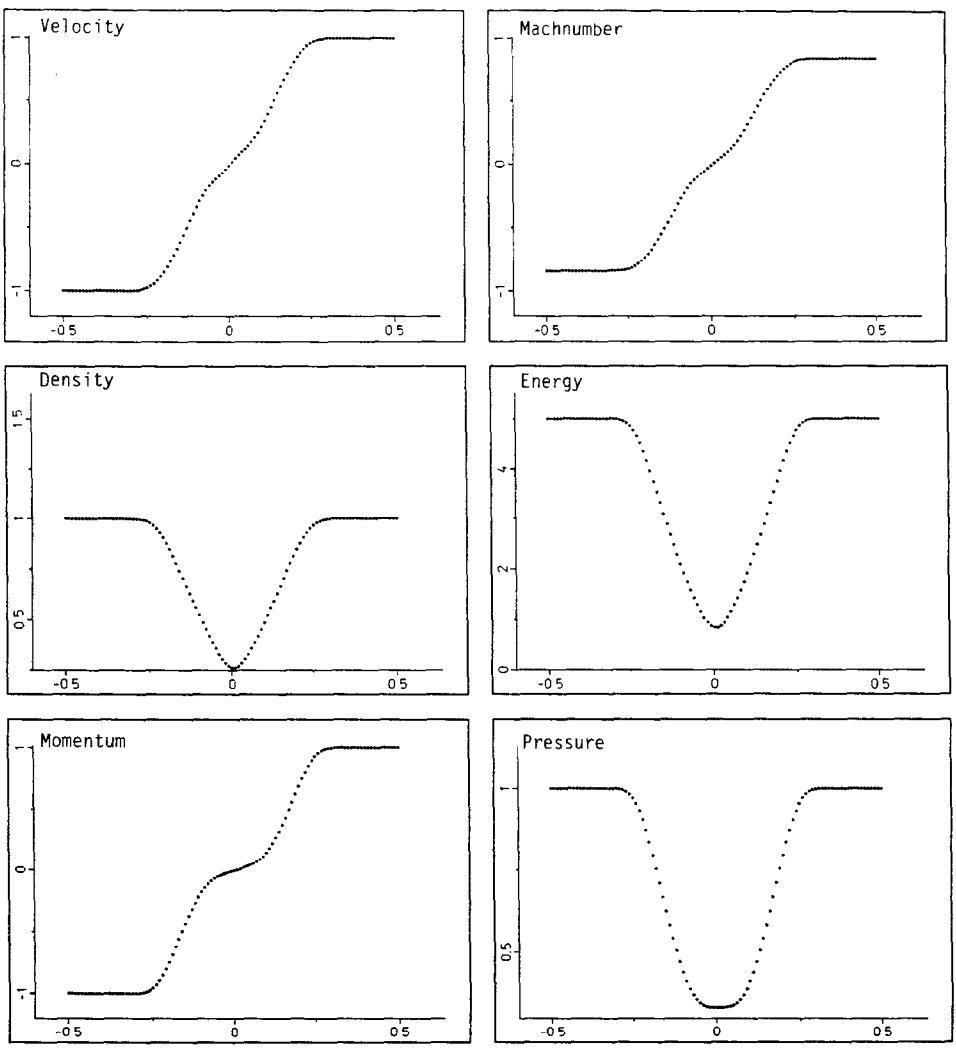

FIG. 6.5. Numerical result of the HLLE-scheme for the 1–1–2–5 problem at time $t = 0.1$.

It follows from (A5) and (A2) that

$$a_r + a_\ell \geqslant u_\ell - u_r. \tag{A6}$$

To ensure positive pressure we need

$$\rho^* e^* - \tfrac{1}{2}(m^{*2} + n^{*2}) \geqslant 0. \tag{A7}$$

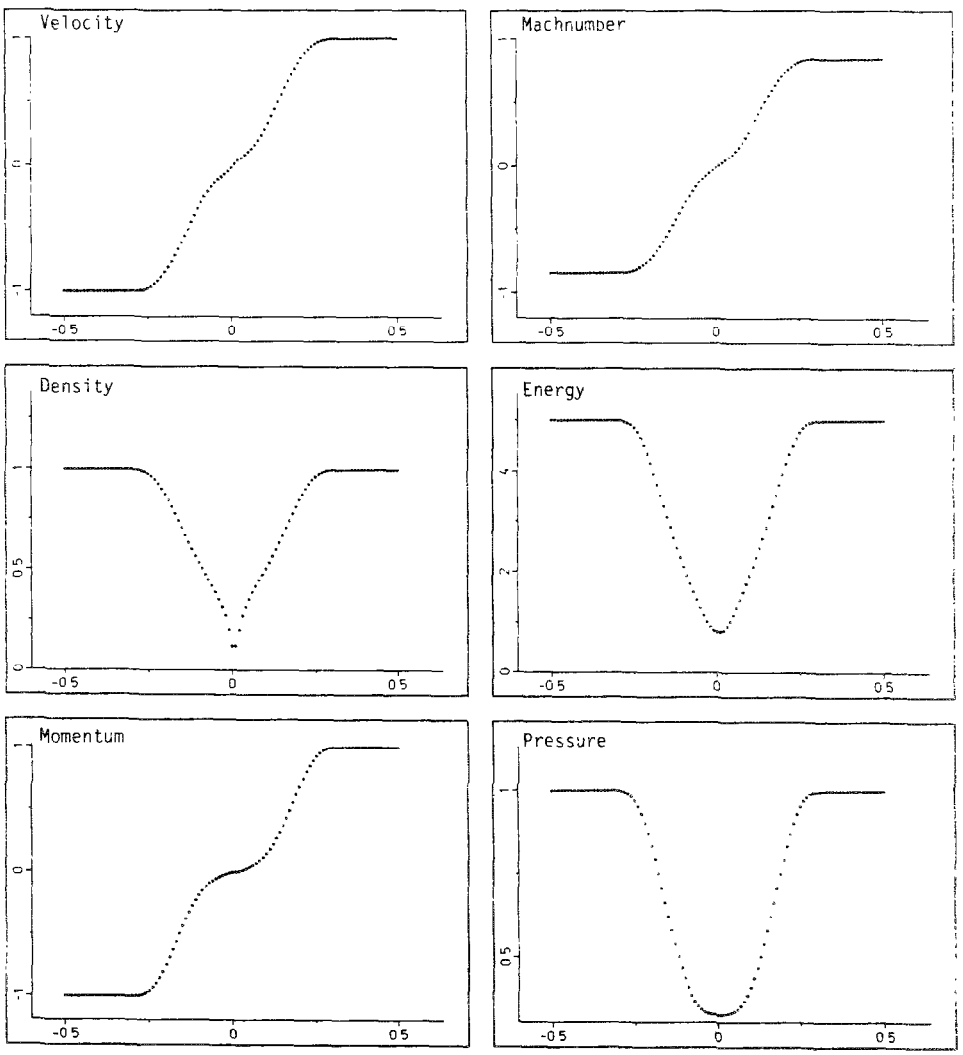

FIG. 6.6. Numerical result of the HLLEM/Roe-scheme for the 1–1–2–5 problem at time $t = 0.1$.

Some algebra shows that this condition is equivalent to

$$\frac{1}{\gamma-1}(a_r\rho_r + a_\ell\rho_\ell)(a_r p_r + a_\ell p_\ell)$$
$$+\frac{1}{2}\rho_\ell\rho_r(u_r-u_\ell)^2 a_\ell a_r + \frac{1}{2}\rho_\ell\rho_r(v_r-v_\ell)^2 a_\ell a_r$$
$$-(a_r\rho_r p_\ell + a_\ell\rho_\ell p_r)(u_r-u_\ell) - \frac{1}{2}(p_r-p_\ell)^2 \geqslant 0. \tag{A8}$$

Condition (A8) defines the exterior of an ellipse or hyperbola in the plane (a_ℓ, a_r). One way to ensure that this condition is always satisfied is to assume $v_r - v_\ell = 0$ (which is the worst case). We then treat the expression as quadratic in $\Delta u = u_r - u_\ell$ and insist that no values of the coefficients give real roots. This condition is

$$(a_r\rho_r p_\ell + a_\ell\rho_\ell p_r)^2 \leqslant -\rho_\ell\rho_r a_\ell a_r (p_r-p_\ell)^2$$
$$+\frac{2}{\gamma-1}\rho_\ell\rho_r a_\ell a_r (a_r p_r + a_\ell p_\ell)(a_r\rho_r + a_\ell\rho_\ell), \tag{A9}$$

which is equivalent to

$$\left(\frac{2}{\gamma-1}\right)\left(\frac{\rho_r\rho_\ell p_r}{a_r}\right)\left(a_r^2 - \frac{\gamma-1}{2}\frac{p_r}{\rho_r}\right)$$
$$+\left(\frac{2}{\gamma-1}\right)\left(\frac{\rho_\ell\rho_r p_\ell}{a_\ell}\right)\left(a_\ell^2 - \frac{\gamma-1}{2}\frac{p_\ell}{\rho_\ell}\right) \geqslant 0. \tag{A10}$$

Condition (A10) is satisfied by

$$a_\ell^2 \geqslant \frac{\gamma-1}{2\gamma}c_\ell^2 \tag{A11a}$$

$$a_r^2 \geqslant \frac{\gamma-1}{2\gamma}c_r^2 \qquad (c \sim \text{sound speed}) \tag{A11b}$$

and these results are the sharpest possible of the form $a_\ell = a(q_\ell)$ and $a_r = a(q_r)$.

REFERENCES

1. M. CRANDALL AND A. MAJDA, *Numer. Math.* **34**, 285 (1980).
2. B. EINFELDT, *SIAM J. Numer. Anal.* **25**, 294 (1988).
3. B. EINFELDT, *Proc. Roy. Soc. London*, submitted.
4. S. K. GODUNOV, *Mat. Sb.* **47**, 271 (1959).

5. A. HARTEN AND M. HYMAN, *J. Comput. Phys.* **235** (1983).
6. A. HARTEN, P. D. LAX, AND B. VAN LEER, *SIAM Rev.* **25**, 35 (1983).
7. A. HARTEN, *J. Comput. Phys.* **49**, 357 (1983).
8. S. OSHER AND S. CHAKRAVARTHY, *SIAM J. Numer. Anal.* **21**, 955 (1984).
9. P. L. ROE, *J. Comput. Phys.* **53**, 357 (1981).
10. J. SMOLLER, *Shock Waves and Reaction-Diffusion Equations* (Springer-Verlag, New York/Berlin, 1983).
11. M. VINOKUR, *J. Comput. Phys.* **81**, 1 (1989).